Available online at www.sciencedirect.com
SCIENCE DIRECT®
Journal of Nuclear Materials 337–339 (2005) 786–790
journal of nuclear materials
www.elsevier.com/locate/jnucmat

Thermographic power accounting in MAST

F. Lott [a,b,*], A. Kirk [b], G.F. Counsell [b], J. Dowling [b], D. Taylor [b], T. Eich [c], A. Herrmann [c]

[a] Plasma Physics Group, Blackett Laboratory, Imperial College London, SW7 2BW, UK
[b] EURATOM/UKAEA Fusion Association, Culham Science Centre, Abingdon, Oxon, OX14 3DB, UK
[c] Max-Planck-Institut für Plasmaphysik, EURATOM Assoziation, D-85740 Garching, Germany

Abstract

Target heat loads calculated from the infrared camera on MAST are presented. A parameter (α) is used to account for surface effects. In L-Mode discharges, the energy arriving at the targets, as calculated from the camera using a suitable choice of α, is in agreement with that calculated from Langmuir probes and that lost from the core. In H-Mode, energy balance can also be achieved both at the ELM and in inter-ELM periods, although a different value of α is required for different targets and for different power loads. This may be due to increased erosion leading to the production of dust in the plasma sheath.

PACS: 52.70.Kz; 52.55.Fa; 52.40.Hf; 87.63.Hg
Keywords: Divertor plasma; ELM; MAST; Power balance; Thermography

1. Introduction

The Mega-Ampère Spherical Tokamak (MAST) has a number of differences from conventional tokamaks. Amongst these is its open design, allowing easy access for plasma diagnostics, particularly those for imaging such as cameras. This enabled the installation of a Santa Barbara Focal-Plane infrared camera, which is a very good tool for power studies. This camera can operate at up to 10 kHz sampling rate making it ideal for studying transient events such as ELMs.

Langmuir probe data can be used to calculate heat loading on MAST's divertor tiles with high spatial and temporal resolution, using the observed ion saturation current and electron temperature (T_e). The ion temperature, T_i, is assumed to be equal to T_e in this calculation. In previous studies on MAST [1], it has been found that using this assumption in L-Mode provides good balance between the power entering the scrape-off layer (SOL) and that measured arriving at the divertor targets by the probes. However, in H-Mode, less power is seen at the targets than predicted. Another diagnostic is therefore needed to determine whether this power is going elsewhere such as the first wall of the vacuum vessel, or whether the probe power is being miscalculated by assuming $T_i = T_e$. There is evidence from ASDEX-Upgrade that considerable power does reach the first wall [2]. The infrared camera was commissioned with the aim of studying power loadings to all in-vessel components, including the first wall.

* Corresponding author. Tel.: +44 1235 466807; fax: +44 1235 466379.
E-mail address: fraser.lott@ukaea.org.uk (F. Lott).

0022-3115/$ - see front matter © 2004 EURATOM/UKAEA. Published by Elsevier B.V. All rights reserved.
doi:10.1016/j.jnucmat.2004.10.053

2. Analysis technique

2.1. Temperature calculations from infrared camera data

The infrared camera measures incoming photon flux, so the first step in computing power deposited on the tile is to convert photon flux at the camera into temperature at a given time and position in the emitting region. The LEON code was developed for this purpose. Containing a model of the interior of MAST, it maps the two-dimensional camera image onto the MAST surfaces where they originated. Given an area of interest (usually that occupied by the probes), the program extracts the data as a function of radial position and time. The temperature profile can then be obtained from the blackbody law.

$$n_{\text{count}} = \frac{c_{\text{phot}}}{e^{\frac{hc}{\lambda k_B T}} - 1} + n_{\text{offset}}.$$

The constants c_{phot} and n_{offset} are found by calibrating against a laboratory blackbody source. Providing LEON with these values, the temperature versus time and position can be calculated.

2.2. Power calculations from temperature

In order to calculate the power flux onto a tile, we must solve the inverse heat equation, utilising the temperature history of the tile to deduce power at a given time. The software used for this is the THEODOR code [3], developed for ASDEX-Upgrade and also used on JET.

The major problem observed with the power profiles produced by THEODOR and other heat solvers is that unphysical negative heat fluxes can be calculated. It was theorised that this effect was due to hydrocarbon layers deposited on the surface of the tile, which would glow brightly during the heat pulse then stop emitting immediately afterwards due to fast conduction into the tile beneath. To alleviate this problem, THEODOR contains a surface parameter, α [4].

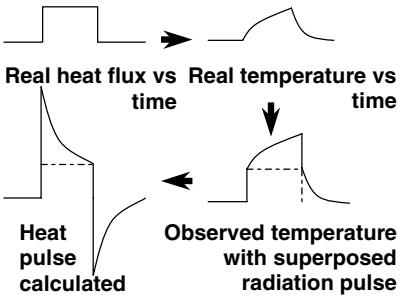

Fig. 1. A simplified diagram of the effects of additional radiation on reverse heat transforms.

$$q = \alpha \Delta T,$$

where q is the heat applied to the surface and ΔT is the difference in temperature between the top surface of the layer and the bulk of the tile. α is the ratio of the heat conductivity to thickness of the layer (in units $\mathrm{Wm^{-2}K^{-1}}$), so it affects the overall heat conduction and apparent brightness of the tile. Adjusting it can reduce or remove negative heat fluxes. A simple diagram of this effect is shown in Fig. 1. Note that care must be taken in choosing α, as a value which is too low results in the data being oversmoothed and the power will be underestimated.

Choosing α can be approached from a number of directions.

1. Reduce the value of α until there are no longer any negative heat fluxes evident in the data.
2. Match the power from the camera with that determined from other diagnostics, such as the Langmuir probes.
3. Plot the total energy received at the divertor during the discharge against α. This gives a curve which flattens as α tends to infinity. An optimal value is found at the knee of the curve, where the removal of negatives is best traded off against loss of peak power. Examples of this kind of plot can be seen in Fig. 2.

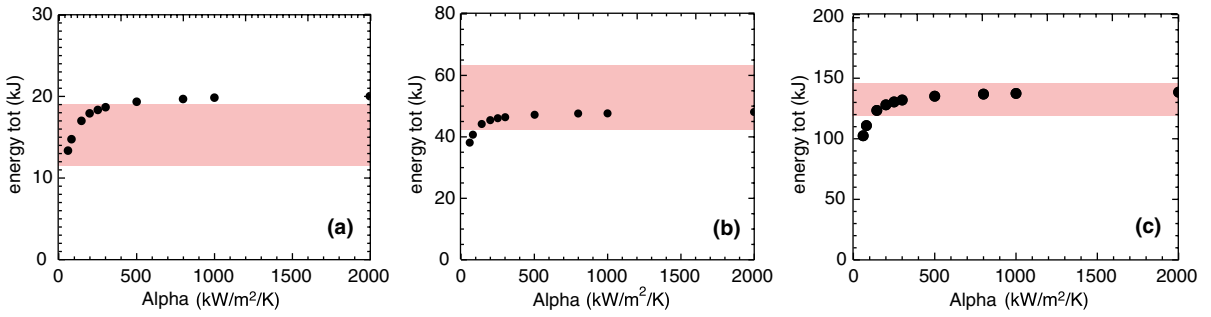

Fig. 2. Summed energy over a discharge vs. α, with probable energy band from probe split shaded. (a) energy to the inner target during a single-null L-Mode plasma (shot 7501). (b) energy to the outer lower target during a double-null L-Mode plasma (shot 7734). (c) energy to the outer lower target during a double-null H-Mode plasma (shot 8812).

4. Compute total conductivity from the exponential drop in temperature after the heat pulse, and extrapolate α from that. In reality, the heat pulses are not the square-wave suggested in Fig. 1, so the drop in temperature is usually too complex to analyse in this way.

3. Results

3.1. L-mode power calculations

Since the power entering the SOL matches that measured by the target probes in L-Mode, this is the ideal mode of operation to test whether agreement can be reached between the camera and other diagnostics. Fig. 3 shows minimum and maximum power density (over the whole radial extent of the data) as a function of time and a variety of values of α. There is clearly a large variation in both the peak and minimum power density at the target. If we follow method 1 (in Section 2.2) for finding optimum α, we discover that although the size of negative pulses decreases with decreased α, they are not completely removed. This makes the value chosen by this method somewhat arbitrary.

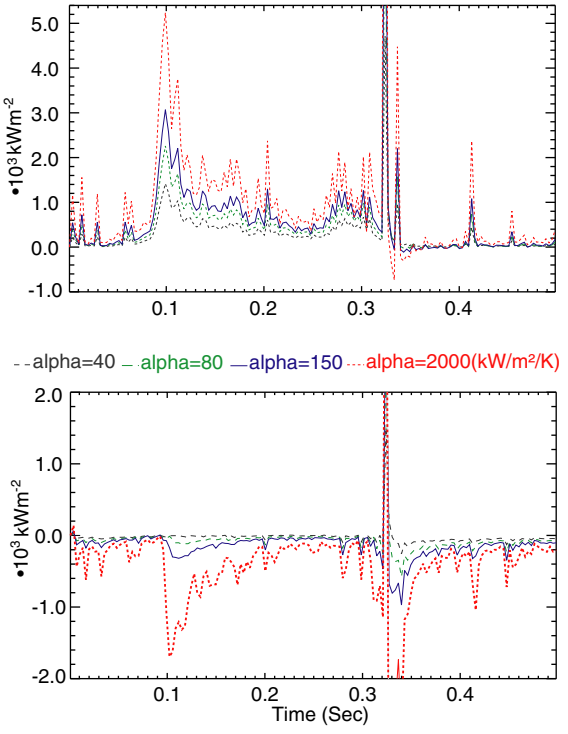

Fig. 3. Maximum (above) and minimum (below) power densities vs. time, for a range of values of α, during an L-Mode discharge (shot 7734).

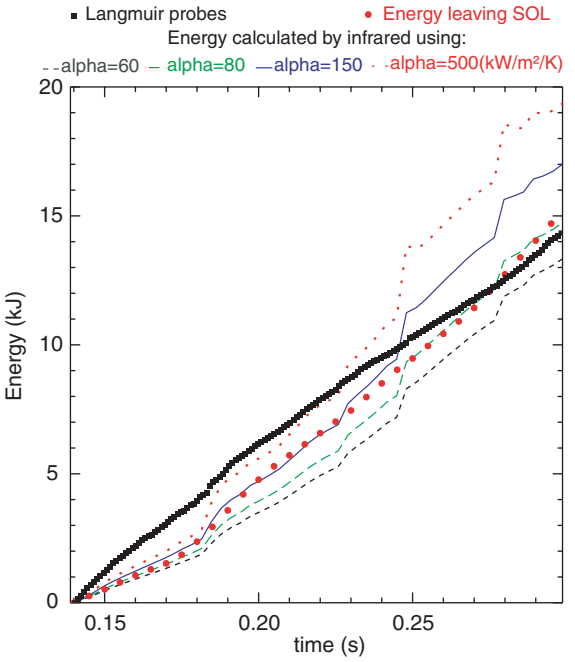

Fig. 4. Summed energy vs. time for an L-Mode plasma (shot 7501), showing SOL energy, probes and infrared data at a range of values of α.

Integrating power arriving at the target over time gives the plot in Fig. 4. Superimposed is an estimate of the energy emitted from the core arriving at this target, calculated from the ratio of energy arriving at different targets as measured by the Langmuir probes, and scaled according to the total change in core energy (with radiation away from the targets, as measured by bolometers, subtracted). This comparison can also be used to determine α (method 2 in Section 2.2). Since there is broad agreement between energy from the core and energy to the probes, we might presume to take an α which gives a similar energy to the other diagnostics, in this case between 80 and 150 $\mathrm{kW\,m^{-2}K^{-1}}$. However, there is an indication that the required value of α varies through the shot. This might indicate that there are changes in surface properties as the shot progresses.

Method 3, the total energy arriving at the inboard target calculated from the camera data against α as shown in Fig. 2, is another possible indicator of optimum α. To verify, we can compare this to the estimated amount of energy emitted from the core arriving at this target (the shaded region in Fig. 2(a)). In order to remove most of the anomalous negative heat fluxes, and be in agreement with the data from the probes and core energy loss, a value of α in the range 60–100 $\mathrm{kW\,m^{-2}K^{-1}}$ is required.

Fig. 2(b) shows the results for the outboard target in L-Mode. Interestingly, the most suitable value of α is

now further up the curve and a number from 100 to $200\,kW\,m^{-2}K^{-1}$ is required. This may indicate that the surface properties are different at the two targets.

3.2. H-mode power calculations

Section 3.1 demonstrates that using α in thermographic calculations can give sensible results under steady-state conditions. Now moving to ELMing H-Mode double-null plasmas, anomalous heat fluxes are increasingly evident.

Fig. 2(c) plots total energy against α with the energy fraction to the target superimposed. It suggests that a value of $\alpha \sim 140\,kW\,m^{-2}K^{-1}$ is appropriate. However, this is not the whole story, as can be seen when the power balance during ELMs and inter-ELM periods are examined independently.

Fig. 5(a) shows target energy calculated from the camera, for three values of α, versus energy from the SOL arriving at that target during inter-ELM periods. A value of $\alpha = 140\,kW\,m^{-2}K^{-1}$ gives good energy accounting. This value is similar to that found at this target for L-mode.

Fig. 5(b) shows a similar plot during ELMs. While the probe data still underestimates the energy leaving the plasma core, the infrared data appears to overestimate the energy for all but very low values of α. This immediately indicates that the required value of α must be different during ELMs to inter-ELM and L-Mode, since $\alpha = 140\,kW\,m^{-2}K^{-1}$ would give us more energy arriving at the targets than is emitted from the plasma. This suggests that whatever causes the excess radiation detected by the camera is much more prominent during ELMs than otherwise.

4. Possible causes of anomalous heat fluxes

Though α is intended to model hydrocarbon layers on the divertor tiles, other factors may produce this kind of effect. Molecular radiation (or other such ambient light) might be produced by an ELM. Since it is not directly associated with thermal emission, it would also produce this a similar signal and both would require THEODOR to produce a negative heat flux to account for the lack of decay curve associated with the cooling of the tile. More recently, non-uniformities in the surface, such as microscopic structure in the carbon tile or dust layers, have been suggested as a possible cause [5,6]. It is suggested that these would give hot-spots on a scale much smaller than the resolution of the camera, such that the temperature is not properly calculated due to the exponential nature of blackbody radiation.

None of these explanations seem entirely satisfactory. Most ambient radiation is eliminated by the narrow wavelength band that the camera observes (this will be studied in future experiments by narrowing the band still further). With regard to surface layers, whether dust or film, it seems surprising that the incident plasma would not immediately remove them, negating their effect, especially during periods of high loading such as ELMs. Further, we might expect non-uniformities in the tile surface to be eroded by exposure to the plasma, since the increased heat loading which could produce the hot-spot effect is more likely to ablate that area than any other part of the tile. This should leave a uniform surface without hot-spots. Further, non-uniformities should be predominant for carbon-fibre composite tiles due to their inherent fibre structure, whereas the tiles in MAST are graphite, and should be more

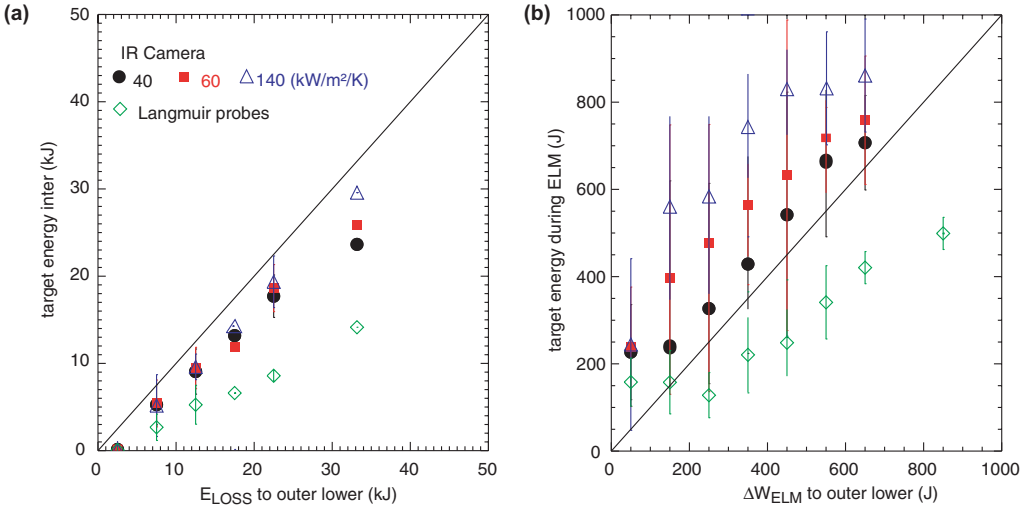

Fig. 5. Power balance between power into the SOL (solid line) and power measured by the Langmuir probes and the camera, compiled over a number of discharges. (a) (left): Inter-ELM energy. (b) (right): ELM energy.

uniform. Nevertheless, an α parameter is still required empirically.

Our suggestion might be considered a hybrid of the above theories. The infrared video shows a considerable quantity of dust thrown up in MAST's target area during a discharge. This dust can survive in the sheath region and is highly radiative [7]. We suggest that this dust forms a surface layer on the tile during low-power parts of the discharge. During high power such as during ELMs, it loosens and is carried in the sheath region, providing extra radiation during these phases which is misinterpreted due to being much smaller than the resolution of the camera. After a length of time the dust will be redeposited or burnt up to become impurities in the plasma. An experiment is being devised to test this hypothesis.

5. Conclusions

The infrared camera is a valuable addition to the diagnostics on MAST. Although infrared measurements can be susceptible to radiation other than that caused by the bulk temperature of the tile, the infra-red camera still produces valid results once this is accounted for using the α parameter. Unlike on other experiments, optimising this parameter does not completely eliminate anomalous heat fluxes, and different values of α are required for high-power events such as ELMs. These factors make producing meaningful results for peak power density difficult, and suggest that surface effects are not the only cause of miscalculation in power profiles from infrared data.

Acknowledgments

This work was funded jointly by the United Kingdom Engineering and Physical Sciences Research Council and EURATOM.

Many thanks to Dr Philip Andrew for useful discussions.

References

[1] A. Kirk et al., Plasma Phys. Control. Fus. 46 (2004) 551.
[2] A. Herrmann et al., Plasma Phys. Control. Fus. 46 (2004) 971.
[3] A. Herrmann et al., Plasma Phys. Control. Fus. 37 (1995) 17.
[4] A. Herrmann et al., in: 28th EPS Conference on Controlled Fusion and Plasma Physics, 2001, Funchal.
[5] A. Herrmann et al., Phys. Scr. T 111 (2004) 98.
[6] E. Delchambre et al., these Proceedings. doi:10.1016/j.jnucmat.2004.10.015.
[7] J. Martin et al., these Proceedings. doi:10.1016/j.jnucmat.2004.08.029.